Aquaculture Reports 38 (2024) 102345

Contents lists available at ScienceDirect

Aquaculture Reports

journal homepage: www.elsevier.com/locate/aqrep

Genetic management of small abalone (*Haliotis diversicolor*) by using ISSRseq technology

Yung-Cheng Chang [a,b], Fan-Hua Nan [a], Te-Hua Hsu [a,b,1,*]

[a] Department of Aquaculture, National Taiwan Ocean University, Taiwan
[b] Center of Excellence for the Oceans, National Taiwan Ocean University, Taiwan

ARTICLE INFO

Keywords:
Next Generation Sequencing
Molecular markers
MIG-seq
SNP
Breeding

ABSTRACT

The small abalone (*Haliotis diversicolor*) is commercially valuable for fisheries and aquaculture. Once ranked first globally, Taiwan's abalone industry is now on the brink of collapse due to disease issues. Despite improvements in survival rates through crossbreeding between Japan and Taiwan populations, the subsequent lack of further breeding selection and genetic management has led to disorder after over a decade of introduction. With frequent commercial exchanges, stock enhancement, private introductions, and hybridization, genetic management of *H. diversicolor* poses both challenges and necessity. This study utilizes ISSRseq technology to aid in the genetic management of *H. diversicolor*. Various analyses show significant differences among the Japan wild population, Taiwan wild populations, the Taiwan-Indonesia hybrid strain, and other cultured populations. Selective strains bred by research institutions and private hatcheries exhibit uniqueness distinct from commercial *H. diversicolor*. The presence of multiple populations exhibiting admixture may be attributed to improper stock enhancement and management practices. Our work elucidates the current status of genetic resources of Taiwan *H. diversicolor*, laying the foundation for future breeding efforts.

1. Introduction

The *Haliotis* genus, the only genus within the Haliotidae family, comprises approximately 67 species worldwide (MolluscaBase, 2024). These species inhabit a diverse range of temperate and tropical coastal reefs and rocky habitats, typically from sea level to depths of 30 m (Geiger, 1999; Degnan et al., 2006). About 14 of these species hold significant economic importance for fisheries and aquaculture, predominantly thriving in temperate seas (Estes et al., 2005; Gao et al., 2023). Notably, compared to the predominantly cultivated abalone species in temperate seas, the *H. diversicolor* is one of the few tropical to subtropical abalone species subjected to large-scale cultivation (You et al., 2009; Hsu and Gwo, 2017). It emerges as a globally significant commercial species, widespread across warm water regions of East Asia, including Indonesia, the Philippines, Taiwan, the southern coastal waters of China, Jeju, Korea, and south Japan (Kuroshio warm water region) (Geiger, 1999; Hsu and Gwo, 2017).

In Taiwan, the *H. diversicolor* represents a valuable commodity in fisheries and aquaculture due to its premium price, rapid growth, and short life cycle (Chen and Lee, 1999; Huang and Hseu, 2010; Hsu and Gwo, 2017). Taiwanese pioneers in *H. diversicolor* aquaculture witnessed rapid commercial expansion in the 1980s, propelled by successful seed production and the development of a unique land-based multiple-tier culture system (Chen and Lee, 1999; Huang and Hseu, 2010; Hsu and Gwo, 2017). From 1993 onwards, annual production soared rapidly, peaking in 2000 at approximately 2500 metric tons with a value exceeding 1.2 billion NTD, leading global production of farmed *H. diversicolor* (FAO, 2000). Besides Taiwan's *H. diversicolor* aquaculture, Taiwanese farmers transplanted broodstock and farming techniques to southern China (Fujian, Guangdong, Guangxi, and Hainan Provinces) in the mid-1980s, spurring a massive expansion of the aquaculture industry along the south of Chinese coasts throughout the 1990s (Nie and Wang, 2004; Zhang et al., 2004; You et al., 2009). By 2001, the estimated output of *H. diversicolor* in southern China reached approximately 3878 tons (Nie and Wang, 2004; Zhang et al., 2004).

However, since 2002, Taiwan and southern China have experienced disease outbreaks and significant mortality among *H. diversicolor* at the postlarval and grow-out stages (Chang et al., 2005; You et al., 2009; Gu et al., 2019). Research attributes the large-scale winter mortality in 2003 to two primary viruses: the Abalone Herpes Virus (AbHV) and the

* Correspondence to: Department of Aquaculture, National Taiwan Ocean University, 2 Beining Road, Jhongjheng District, Keelung City 20224, Taiwan.
E-mail address: realgigi@mail.ntou.edu.tw (T.-H. Hsu).
[1] https://orcid.org/0000–0001-7819–4122

https://doi.org/10.1016/j.aqrep.2024.102345
Received 11 April 2024; Received in revised form 21 August 2024; Accepted 5 September 2024
Available online 11 September 2024

Abalone Shriveling Syndrome-associated Virus (AbSV) (Chang et al., 2005; Chen et al., 2012, 2014; Jiang et al., 2012). To enhance survival rates, crossbreeding individuals from different regions (Taiwan and Japan) is helpful (You et al., 2009). Thus, around 2010, *H. diversicolor* was imported from Japan for crossbreeding to increase genetic diversity and alleviate winter mortality issues (You et al., 2009; Hsu and Gwo, 2017). However, after several years of development, although there was a slight improvement in production, the introduction of wild individuals led to a decline in growth and an issue of poor environmental adaptation. Starting from 2003, the Taiwan abalone industry suffered a significant downturn due to disease issues, with annual production plummeting to less than 40 metric tons by 2013, subsequently remaining below 300 tons (FAO, 2000; Hsu and Gwo, 2017). The Taiwan abalone industry is now facing imminent collapse. Meanwhile, China's abalone aquaculture has shifted predominantly to disc abalone and its hybrids, with production expanding rapidly to 200,000 tons over the past two decades (Gao et al., 2023).

Due to a lack of knowledge and technical expertise in genetic management among aquaculture operators, genetic resources have become disorganized after more than a decade of introducing Japanese populations to crossbreeding. To further improve survival and growth rates in cultured *H. diversicolor*, breeding program efforts must be guided by insights from genetic analyses into the population origins, the genetic introgressions, and the genetic health of the different strains. In the management of genetic resources, molecular markers play a crucial role. Molecular markers are DNA segments associated with specific genes or traits, allowing researchers to identify and select individuals with desirable characteristics and differentiate between various strains, populations, and species (Hsu et al., 2011; Hsu et al., 2020a, 2020b). They have become indispensable tools in fisheries and aquaculture research (You et al., 2020; Hsu et al., 2022; Wong et al., 2022).

In recent years, high-throughput next-generation sequencing (NGS) technologies have significantly advanced molecular marker-assisted breeding by facilitating the rapid identification and genotyping of numerous molecular markers. One such NGS-based technique is MIG-seq (Multiplexed Inter-simple Sequence Repeat Genotyping by Sequencing; Suyama and Matsuki, 2015), also known as ISSRseq technology (Sinn et al., 2022). MIG-seq is an effective PCR-based genome-wide method for single-nucleotide polymorphism (SNP) genotyping using the next-generation sequencing platform. It has been successfully applied to assist growth selection in tomato groupers and holds promise for enhancing genetic management in various aquaculture species (Onuki and Fuke, 2022; Hsu et al., 2024).

While one-on-one mating is feasible, commercial breeding primarily relies on large-scale reproduction. These species often encounter challenges in frequent commercial exchanges, wild releases, undisclosed introductions, and hybridization, leading to difficulties and the necessity of genetic management. Due to the expected minor differences among various genetic resources, it is essential to employ next-generation sequencing to obtain more detailed and comprehensive analytical

Table 1
Genetic diversity of 255 individuals from 19 populations of *H. diversicolor*.

clade	*n*	Loci	variant sites	π	*Ho*	*He*	F_{IS}	Clade*	source
P-CI	10	731	1138	0.282	0.232	0.263	0.099	1	Private breeding program
P-CL	8	1313	1680	0.299	0.313	0.276	-0.098	1	(Commercial Hatchery, Miao-li)
P-CJ	10	796	1464	0.279	0.237	0.261	0.057	2	
P-CK	15	1582	2619	0.276	0.254	0.258	0.075	2	
P-CU	24	472	912	0.173	0.171	0.168	0.028	2	
S-JH	14	1084	1724	0.234	0.238	0.224	-0.018	3	Commercial hatchery (seeds)
S-LC	10	1474	2071	0.289	0.296	0.27	-0.052	3	
S-WG	10	1361	1995	0.27	0.259	0.252	-0.007	3	
S-XW	10	868	1285	0.283	0.261	0.264	0.019	4	
F-CM	10	534	747	0.276	0.256	0.257	0.013	4	Commercial farm (mass production)
F-LS	11	951	1344	0.253	0.27	0.239	-0.081	4	
F-ND	22	589	1148	0.165	0.164	0.16	0.018	4	
F-WI	10	896	1225	0.282	0.288	0.264	-0.039	4	
H-XH	10	983	1202	0.316	0.183	0.296	0.37	5	Taiwan-Indonesia hybrid strain
R-SB	24	391	561	0.187	0.207	0.182	-0.058	6	Research program (New Taipei City)
R-NU	20	793	1295	0.196	0.211	0.19	-0.034	7	Research program (NTOU 108)
W-TD	8	1730	2727	0.296	0.279	0.273	-0.014	4	Wild, Tai-tung,Taiwan
W-TI	10	1294	2422	0.255	0.223	0.238	0.046	4	Wild, I-lan, Taiwan
W-JP	24	952	2827	0.129	0.125	0.126	0.026	8	Wild, Wakayama, Japan
All	255	550	2394	0.076	0.067	0.076	0.096	—	—

*Denoting eight clades based on STRUCTURE analysis.

results. This study utilizes ISSRseq technology to aid in genetically managing *H. diversicolor*, including wild, commercial, and research populations from Taiwan. A comparison was made with wild samples from Japan to elucidate the current status of *H. diversicolor* genetic resources in Taiwan and lay the groundwork for future breeding efforts.

2. Material and methods

2.1. Sample preparation and DNA extraction

A total of 255 specimens of *H. diversicolor* were used in this study (Table 1). Fresh specimens were obtained from 2021 to 2022, including five private breeding program populations (strains) (P-CI, P-CL, P-CJ, P-CK, and P-CU; Commercial Hatchery, Miao-li), four commercial hatchery samples (S-JH, S-LC, S-WG, and S-XW), four commercial farm samples (F-CM, F-LS, F-ND, and F-WI), one hybrid population (strain) (Not F1, source from Taiwan (♀)-Indonesia(♂)), two research breeding program populations (strains) (R-SB, New Taipei City; R-NU, NTOU 108, National Taiwan Ocean University), two wild populations from Taiwan (W-TD, Tai-tung and I-lan, W-TI) and one wild population from Japan (Wakayama, Japan) (Table 1). Small pieces of muscle tissues (about 3–5 mm) were prepared from fresh (use of 2 % alcohol for anesthesia) or frozen samples transported to the laboratory for molecular studies and preserved in 95 % ethanol. A tissue DNA extraction kit (AxyPrep™ Multisource Genomic DNA Miniprep Kit, Axygen Biosciences, Inc., USA) was used to extract genomic DNA from the tissue of each sample according to the manufacturer's protocol. Moreover, 0.8 % agarose gel electrophoresis was performed to assess DNA template quality.

2.2. DNA library preparation

MIG-seq, or ISSRseq, is a PCR-based technique that uses multiplexed inter-simple sequence repeat (ISSR) primers to construct reduced representation libraries (Sinn et al., 2022). Our procedure adhered to the primary steps delineated by Suyama and Matsuki (2015), albeit with minor adjustments. To mitigate instability stemming from PCR amplification, we conducted three PCR replicates for each sample, subsequently consolidating them for a singular PCR cleanup procedure using the QIAquick 96 PCR purification kit (Qiagen; elution volume of 60 μL). Amplification of samples was verified through agarose gel electrophoresis (2 % w/v). Then, PCR products were combined and quantified using the Qubit dsDNA HS Assay before proceeding with library preparation, which adhered to the Illumina DNA PCR-Free Library Prep protocol. Subsequently, the library underwent sequencing using a 300-cycle S4 kit on the NovaSeq 6000 platform (paired-end 150-bp reads, PE150) following the NovaSeq XP workflow. All aspects of library preparation, sequencing, and base calling were conducted by Genomics BioSci & Tech (https://www.genomics.com.tw, accessed on 1 April 2024).

2.3. SNP genotyping

The general quality of the NovaSeq reads underwent assessment through FastQC (Andrews, 2010). Within the raw sequence data, adapter sequences and low-quality tails (quality score ≤ 10) underwent trimming using Trimmomatic 0.32 (Bolger et al., 2014). Sequencing reads underwent filtration to eliminate those shorter than 150 bp. Subsequently, the remaining reads underwent demultiplexing for different individuals via Cutadapt 3.4 (Martin, 2011), which also eliminated reads featuring ambiguous sites (Ns) or those displaying atypical and excessively short lengths compared to the anticipated size of the PCR amplicons. Additionally, primer clipping and length control of reads were executed using Cutadapt 3.4 (Martin, 2011).

The Stacks-2.64 software is extensively employed in RAD-seq data analysis (Rochette et al., 2019). Parameter settings predominantly adhered to default values, with parameter testing conducted following the methodology outlined by Paris et al. (2017). Ustacks, a component of the Stacks package, was utilized to cluster the reads for each sample, where each stack represented an enzyme cutting site (locus). The clustering parameters were set to -m = 3 and -M = 6 (Paris et al., 2017). Subsequently, statistical analysis was conducted on each sample's loci and locus sequencing depth. Following this, Cstacks merged the loci from all samples across different sample loci to generate the catalog consensus sequence for each locus (-n = 4). Sstacks were subsequently utilized, with the minor allele frequency (MAF) set to 0.05 (Rochette et al., 2019). Loci in each sample that deviated from the catalog consensus sequence were identified, and populations were filtered to obtain the SNPs. Only loci shared by more than 50 % (all samples) and 80 % (each population) of individuals were retained for further analysis.

2.4. Population genetic analysis

Genetic diversity parameters, including observed heterozygosity (*Ho*), expected heterozygosity (*He*), genetic differentiation (F_{ST}), the inbreeding coefficient (F_{IS}), and nucleotide diversity (π), were assessed using Stacks-2.64 (Rochette et al., 2019).

Hierarchical analysis of molecular variance (AMOVA) was conducted to dissect the total genetic variance within and between regions utilizing Arlequin 3.5 (Excoffier and Lischer, 2010). Permutations (9999 iterations) of elements between and within regions were performed using F_{ST}-statistics to facilitate comparisons across different groupings. The optimal grouping was automatically determined using SAMOVA (Dupanloup et al., 2002).

Population structure analysis and genetic differentiation examination were conducted to evaluate genetic variation. The R package poppr was utilized to compute a distance matrix and generate a heatmap (Kamvar et al., 2014). Discriminant Analysis of Principal Components (DAPC) was performed using the R package adegenet (Jombart and Ahmed, 2011). A phylogenetic tree was also constructed using the R package SambaR (euclidean distance and F_{ST} method) to investigate sample relationships (de Jong et al., 2021). The phylogenetic tree visualization was carried out using iTOL v6 (Letunic and Bork, 2021).

Compared to Structure, Admixture software provides a more rapid estimation of the ancestral components of individuals (Alexander et al., 2009). Thus, ADMIXTURE software was employed to explore various numbers of putative clusters (ranging from 1 to 10) and compute the ten-fold cross-validation error to determine the most suitable number of clusters (Alexander et al., 2009). Best clustering results for *H. diversicolor* populations based on four supervised methods, including Median-of-Median (MedMed K), Median-of-Mean (MedMean K), Max-of-Median (MaxMedK), and Max-of-Mean (MaxMeaK) (Puechmaille, 2016; Li and Liu, 2018). Summation of the STRUCTURE results by using CLUMPAK (Kopelman et al., 2015; Li and Liu, 2018). The graphical representation of the structure analysis results was achieved using Structure Plot version 2.0 (Ramasamy et al., 2014).

Pairwise relatedness (unrelated, half-sibling, full-sibling) between each pair of individuals was calculated using RELATED (Pew et al., 2015) and Wang's estimator (Wang, 2002). The expected relatedness values (r) were set to 0.5 for full-sibling pairs, 0.25 for half-sibling pairs, and 0 for unrelated individuals (Pew et al., 2015). A relatedness network was constructed based on pairwise relatedness (r) exceeding 0.1, indicating related individuals (Hsu et al., 2022, 2024). The graphical representation was generated using Gephi v0.9 (Bastian et al., 2009). Assessment of the gene flow patterns between populations was carried out using the divMigrate-online and Nm method (Sundqvist et al., 2016).

3. Results

Utilizing ISSRseq, raw reads were obtained from 255 *H. diversicolor* individuals. Post-trimming of barcodes and filtering 251,662,792 high-quality clean reads were obtained. The count of clean reads per

individual displayed variation, ranging from 150,220 to 2742,087, with an average of 986,913 reads. Subsequently, employing the de novo procedure in Stacks (gstacks), 48,136,417 reads were utilized, ranging from 34,906 to 473,836 per sample, with an average of 188,770 reads. Eventually, 1066 to 10,844 loci were retained, averaging 4532 loci. Effective per-sample coverage: mean = 50.7x, stdev = 7.9x, min = 30.6x, max = 75.4x. All loci were retained for subsequent analysis.

The genetic diversity parameters were assessed across 19 populations, yielding the following statistical outcomes: the number of loci ranged from 391 to 1730; the count of variant sites (SNPs) varied between 561 and 2827; nucleotide diversity (π) spanned from 0.076 to 0.316; the inbreeding coefficient (F_{IS}) ranged from −0.098–0.37; observed heterozygosity (*Ho*) of individuals ranged from 0.067 to 0.313; and expected heterozygosity (*He*) of individuals ranged from 0.076 to 0.296 (Table 1). The heatmap visually depicted the pairwise genetic distances among *H. diversicolor* individuals, ranging from 0.001 to 0.061. Generally, the heatmap revealed low differences within populations and substantial differences among populations, particularly highlighting the dissimilarities of population H-XH, W-TD, and W-JP compared to other populations (Fig. 1).

In the Analysis of Molecular Variance (AMOVA), the majority of the variance (73 %) arises from within populations, with a smaller portion (27 %) attributed to among-population differences. The overall F_{ST} value is 0.272 (P = 0 < 0.001), indicating significant differentiation among populations (Table 2). Employing SAMOVA for automatic clustering, the highest supported result is K = 2 (F_{CT} = 0.265), yielding the following clusters: (P-CI, P-CJ, P-CK, P-CL, F-CM, P-CU, S-JH, W-JP, S-LC, F-LS, F-ND, R-NU, R-SB, W-TI, S-WG, F-WI, H-XH, S-XW); W-TD (Table 3). Additionally, the second-highest supported result is K = 17 (F_{CT} = 0.197), with the following clusters: (P-CI, F-CM); (P-CJ, P-CU); P-CK; P-CL; S-JH; W-JP; S-LC; F-LS; F-ND; R-NU; R-SB; W-TI; W-TD; S-WG; F-WI; H-XH; S-XW (Table 3). Although these results are consistent with Fig. 1, they do not provide resolution regarding relationships among populations. Notably, lower support is obtained when manually testing clustering with k = 4 and k = 8 (F_{CT} = 0.114 and 0.014, respectively).

Structure analysis was employed to assess the clustering relationship of the samples (Fig. 2a). The optimal clustering outcomes, supported by the highest consistency, were observed for k = 8 (MedMed and MedMean method), k = 13 (MaxMedK), and k = 11 or 12 (MaxMea), respectively (Fig. 2b). However, considering the integration of results from 20 independent simulations using CLUMPAK, k = 8 yielded the most stable outcome (19/20) (Fig. 2c). Hence, k = 8 was selected for further extended analysis and discussion. Based on the outcomes of the Structure analysis, a general categorization into 8 clusters was discerned: (P-CI and P-CL); (P-CJ, P-CK, and P-CU); (S-JH, S-LC, and S-WG); (F-CM, F-LS, F-ND, F-WI, S-XW, W-TD, and W-TI); H-XH; R-SB; R-NU; W-JP. Despite some inconsistencies observed within specific populations. For instance, P-CK, S-WG, F-CM, F-ND, F-WI, W-TI, and W-TD exhibited noticeable admixture (Fig. 2a).

Discriminant Analysis of Principal Components (DAPC) further presents the optimal clustering outcomes. DAPC distinctly separated the H-XH and W-JP populations from the rest. While the remaining populations exhibited minor spatial distribution differences, they also support the clustering outcomes from STRUCTURE (Fig. 3). In analyzing the phylogenetic tree, notable disparities emerged between the results derived from the Euclidean distance and F_{ST} pairwise matrices. The phylogenetic tree constructed using Euclidean distance highlighted significant distinctions between W-TD and H-XH compared to other populations, aligning with Fig. 1 (Fig. 4). However, this observation does not correspond with the clustering outcomes from STRUCTURE. Conversely, the Fst outcomes revealed substantial differences between H-XH and W-JP relative to other populations (Fig. 5). This finding resonates with the findings from DAPC analysis and corroborates the clustering results from STRUCTURE.

Although DAPC and the phylogenetic tree (based on F_{ST}) yield more consistent clustering results with the STRUCTURE analysis, these analyses primarily operate at the population level. Further insights into the relatedness among individuals can be gained through a Relatedness network analysis using the best clusters (Fig. 3c). When we present relatedness values (r) > 0.1, all samples in the network exhibit a relatedness relationship (Fig. 6). From a spatial perspective, W-JP exhibits the most significant distinct, while R-NU, R-SB, H-XH, and W-TD are located at the periphery of all individuals and appear more cohesive (Fig. 6). Additionally, individuals in the center do not exhibit complete clustering with others from the same population (e.g., F-ND, F-LS), consistent with the admixture observed among individuals from specific

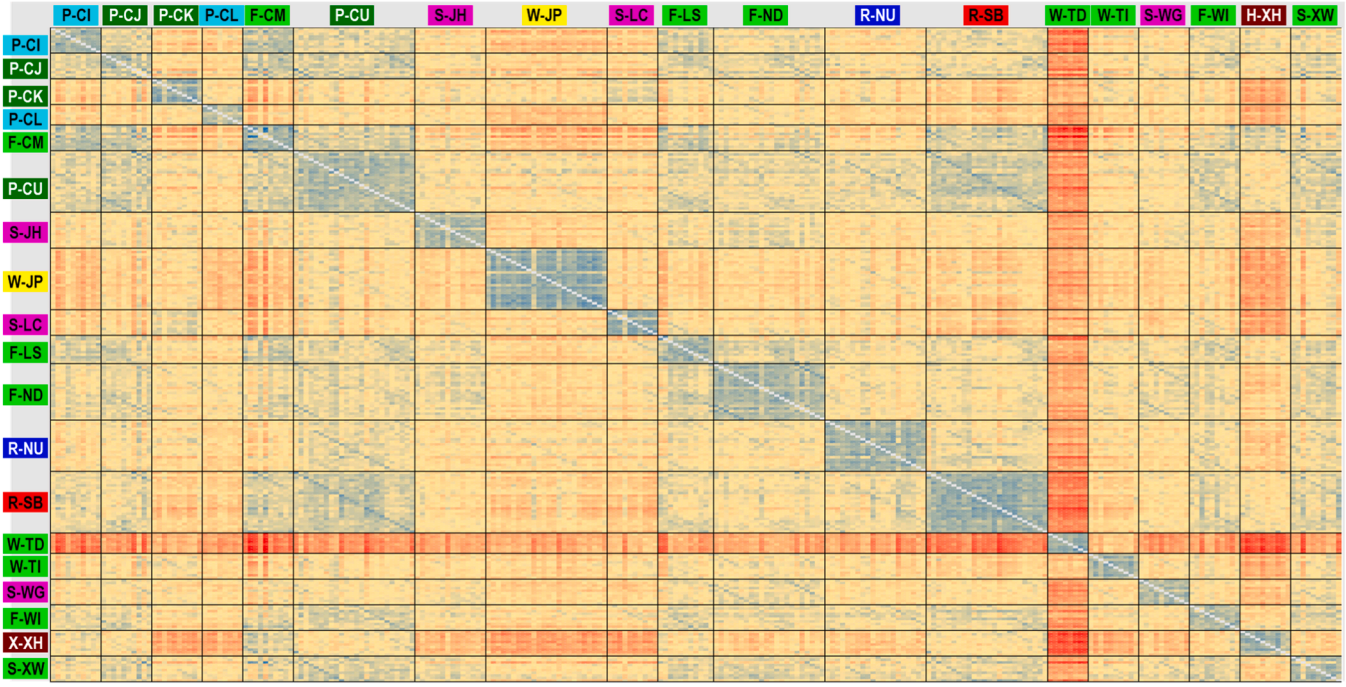

Fig. 1. The genetic distance matrix heatmap of 255 individuals of *H. diversicolor*.

Table 2
Analysis of molecular variance (AMOVA) among all *H. diversicolor* populations.

Source	df	Sum of squares	Mean squares	Variance components	Percentage of variation
Among populations	18	230705.761	12816.987	802.962	27 %
Within populations	236	507733.141	2151.412	2151.412	73 %
Total	254	738438.902		2954.374	100 %

Overall F_{ST} value = 0.272 ($P = 0 < 0.001$)

Table 3
The optimal grouping results of 19 *H. diversicolor* populations. K was automatically determined using SAMOVA.

K	Best grouping results by SAMOVA	F_{CT}
2	(P-CI, P-CJ, P-CK, P-CL, P-CU, S-JH, S-LC, S-WG, S-XW, F-CM, F-LS, F-ND, F-WI, H-XH, R-NU, R-SB, W-TI, W-JP); W-TD	0.265
3	(P-CI, P-CJ, P-CK, P-CL, P-CU, S-JH, S-WG, S-XW, F-CM, F-LS, F-ND, F-WI, H-XH, R-NU, R-SB, W-TI, W-JP); S-LC, W-TD	0.183
4	(P-CI, P-CJ, P-CK, P-CL, P-CU, S-JH, S-LC, S-WG, S-XW, F-LS, F-ND, F-WI, H-XH, R-NU, R-SB, W-TI); F-CM; W-JP; W-TD	0.121
4*	(P-CI, P-CJ, P-CK, P-CL, P-CU, S-JH, S-LC, S-WG, S-XW, F-CM, F-LS, F-ND, F-WI, R-NU, R-SB); H-XH; W-JP; (W-TD, W-TI)	0.114
5	(P-CJ, P-CK, P-CL, P-CU, S-JH, S-XW, F-CM, F-LS, F-ND, F-WI, H-XH, R-NU, R-SB, W-TI); P-CI; W-JP; S-LC; W-TD; S-WG	0.125
6	(P-CI, P-CJ, P-CL, P-CU, S-JH, S-WG, F-CM, F-LS, F-ND, F-WI, H-XH, R-NU, R-SB, W-TI); (P-CK, S-LC); W-TD; W-JP; S-XW	0.123
7	(P-CI, P-CJ, F-CM, P-CU, S-JH, F-LS, F-ND, R-NU, R-SB, S-WG, F-WI, H-XH, S-XW); P-CK; F-CL; W-JP; S-LC; W-TD; W-TI	0.149
8	(P-CJ, P-CU, S-JH, F-LS, F-ND, R-NU, R-SB, S-WG, F-WI, H-XH, S-XW); (P-CI, F-CM); P-CK; P-CL; W-JP; S-LC; W-TD; W-TI	0.135
8*	(P-CI, P-CL); (P-CJ, P-CK, P-CU); (S-JH, S-LC, S-WG); (F-CM, F-LS, F-ND, F-WI, S-XW, W-TD, W-TI); H-XH, R-SB, R-NU, W-JP	0.014
9	(P-CJ, P-CU, S-JH, F-LS, F-ND, R-NU, R-SB, S-WG, F-WI); (P-CI, F-CM); (P-CK, P-CL); W-JP; S-LC; W-TD; W-TI	0.129
10	(P-CJ, P-CU, F-LS, F-ND, R-NU, R-SB, F-WI); (P-CI, F-CM); (P-CK, P-CL); (H-XH, S-XW); S-JH; W-JP; S-LC; W-TI; W-TD; S-WG	0.122
11	(P-CL, S-JH, F-LS, F-ND); (P-CU, R-SB, F-WI); (P-CI, P-CJ, F-CM); (H-XH, S-XW); P-CK; W-JP; S-LC; R-NU; W-TI; W-TD; S-WG	0.119
12	(P-CJ, P-CU, F-WI, H-XH, S-XW); (P-CI, F-CM); (P-CK, P-CL); (F-LS, F-ND); S-JH; W-JP; S-LC; R-NU; R-SB; W-TI; W-TD; S-WG	0.123
13	(P-CI, F-CM, P-CJ, P-CU, F-WI); (F-LS, F-ND); (P-CK, P-CL); S-JH; W-JP; S-LC; R-NU; R-SB; W-TI; W-TD; S-WG; H-XH; S-XW	0.138
14	(P-CI, F-CM, P-CJ, P-CU, F-WI); (F-LS, F-ND); P-CK; P-CL; S-JH; W-JP; S-LC; R-NU; R-SB; W-TI; W-TD; S-WG; H-XH; S-XW	0.153
15	(P-CI, F-CM, P-CJ, P-CU); (F-LS, F-ND); P-CK; P-CL; S-JH; W-JP; S-LC; R-NU; R-SB; W-TI; W-TD; S-WG; F-WI; H-XH; S-XW	0.157
16	(P-CI, F-CM); (P-CJ, P-CU); (F-LS, F-ND); P-CK; P-CL; S-JH; W-JP; S-LC; R-NU; R-SB; W-TI; W-TD; S-WG; F-WI; H-XH; S-XW	0.171
17	(P-CI, F-CM); (P-CJ, P-CU); P-CK; P-CL; S-JH; W-JP; S-LC; F-LS; F-ND; R-NU; R-SB; W-TI; W-TD; S-WG; F-WI; H-XH; S-XW	0.197
18	(P-CI, F-CM); P-CJ; P-CK; P-CL; P-CU; S-JH; W-JP; S-LC; F-LS; F-ND; R-NU; R-SB; W-TI; W-TD; S-WG; F-WI; H-XH; S-XW	0.190

* Manual grouping

populations in STRUCTURE (Fig. 2a).

Gene flow patterns between eight major populations (clades) were estimated using divMigrate-online (Fig. 7) based on the results of the STRUCTURE analyses. Gene flow was greater among six populations ($Nm > 0.5$ between P-CU, R-NU, R-SB, W-TD, S-LC, and W-JP; Fig. 7b), whereas analyses detect lower connectivity between P-CI and H-XH with other populations ($Nm > 0.3$ but < 0.5; Fig. 7b). This result further reflects the gene flow relationship between several major clades, and the high degree of gene flow also shows that the exchanges between the populations in the *H. diversicolor* are frequent.

4. Discussion

This study investigated the genetic diversity and population structure of 255 *H. diversicolor* individuals across 19 populations using ISSRseq genotyping. Analysis of the inbreeding coefficient (F_{IS}), observed heterozygosity (*Ho*) and expected heterozygosity (*He*) revealed that private breeding program strains (P-CI, P-CL, P-CJ, and P-CK) display higher genetic diversity compared to samples from commercial hatcheries and farms, indicating they have not experienced a higher level of genetic bottlenecking. Conversely, research breeding program strains (R-SB and R-NU) exhibit relatively higher levels of purification, though there is still considerable potential for improvement. Interestingly, despite originating from wild populations, samples from Japan exhibit lower diversity (*He* = 0.126) than those from Taiwan, while the H-XH hybrid strains demonstrate higher diversity (*He* = 0.296). These findings highlight significant genetic diversity among the sampled populations, suggesting substantial potential for breeding programs (Table 1). The sample size for certain populations in this study is small (n = 8–10), possibly leading to genetic diversity inaccuracy (e.g., *He*). Furthermore, we observed that higher sample sizes often correspond with lower *He* values. Theoretically, aggregating all samples and covering individuals from more diverse sources would yield higher *He* values. However, we observed the lowest *He* values instead. The main reason is that the proportion of shared loci needs to be adjusted when more samples are included. Generally, as the sample size increases, more individuals may lack common loci, thus lowering the proportion of shared loci. Although this study only retained loci shared by more than 50 % (all samples) and 80 % (each population) of individuals for further analysis, it might be necessary to adjust this threshold to a lower value. The choice of analytical parameters for RADseq and similar technologies has been extensively discussed beyond the sample size. We adhered to the r80 principle in our preliminary analyses, reducing the potential inaccuracy (Paris et al., 2017).

In the commercial production of *H. diversicolor* in Taiwan, operators often require a substantial number of female abalone to ensure an adequate supply of fertilized eggs. In contrast, the demand for male abalones is comparatively lower, with only one-tenth of the breeding stock needed to obtain enough sperm. However, due to asynchronous spawning or spawning by immature individuals, as well as variations in egg quality, unintended genetic drift and bottleneck may occur despite the involvement of many individuals in each artificial fertilization and spawning event (Li et al., 2007; Slabbert et al., 2009; An et al., 2011; Aguilar-Espinoza et al., 2014; Chen et al., 2017). The F_{IS} index shows that only H-XH has a relatively high value ($F_{IS} = 0.37$), while the other populations have values below 0.1, with most even showing negative values. This indicates that the genetic diversity of farmed abalone in Taiwan remains relatively high, and there is no evidence of inbreeding, comparable to that of wild populations. This is partly because private breeding programs in Taiwan have not employed family selection methods or intensive selection, resulting in limited gene purification. Additionally, the past introduction of wild populations from Japan and the partial introduction of wild populations from Indonesia have contributed to maintaining higher diversity levels in farmed abalone populations in Taiwan (Hsu and Gwo, 2017). In many abalone hatcheries, information about broodstock is frequently scarce, particularly when individual abalone lacks proper labeling. Moreover, seedling mix-ups can occur, leading to difficulties in managing genetic resources effectively. For example, we observed mixed clades within populations P-CK and S-WG. Therefore, continuously monitoring genetic diversity and inbreeding levels within cultured populations is crucial (Li et al., 2007; Slabbert et al., 2009; An et al., 2011; Aguilar-Espinoza et al., 2014; Chen et al., 2017).

The STRUCTURE analysis revealed eight distinct clades, corroborated by DAPC and phylogenetic tree analyses (Figs. 2, 3, and 5).

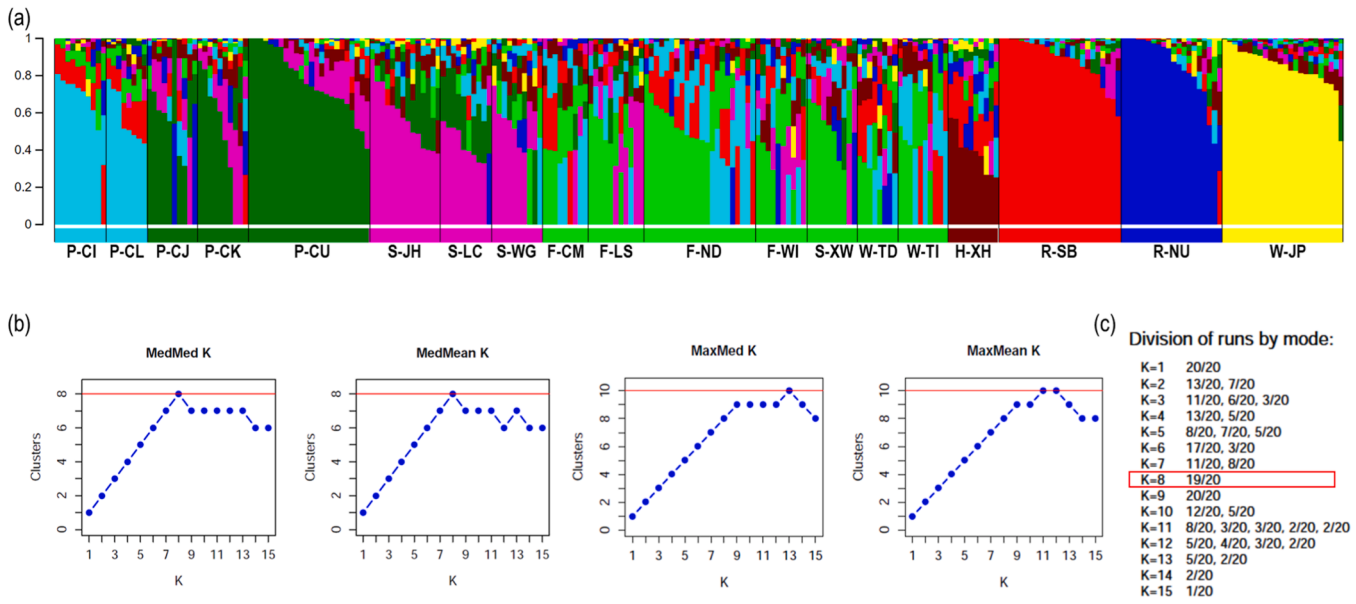

Fig. 2. STRUCTURE analysis of 19 *H. diversicolor* populations. (a) Best clustering results for *H. diversicolor* populations (K = 8). (b) Estimated number of clusters (K) based on four supervised methods including Median-of-Median (MedMed K), Median-of-Mean (MedMean K), Max-of-Median (MaxMed K), and Max-of-Mean (MaxMea K). (c) Summation of the STRUCTURE results by using CLUMPAK.

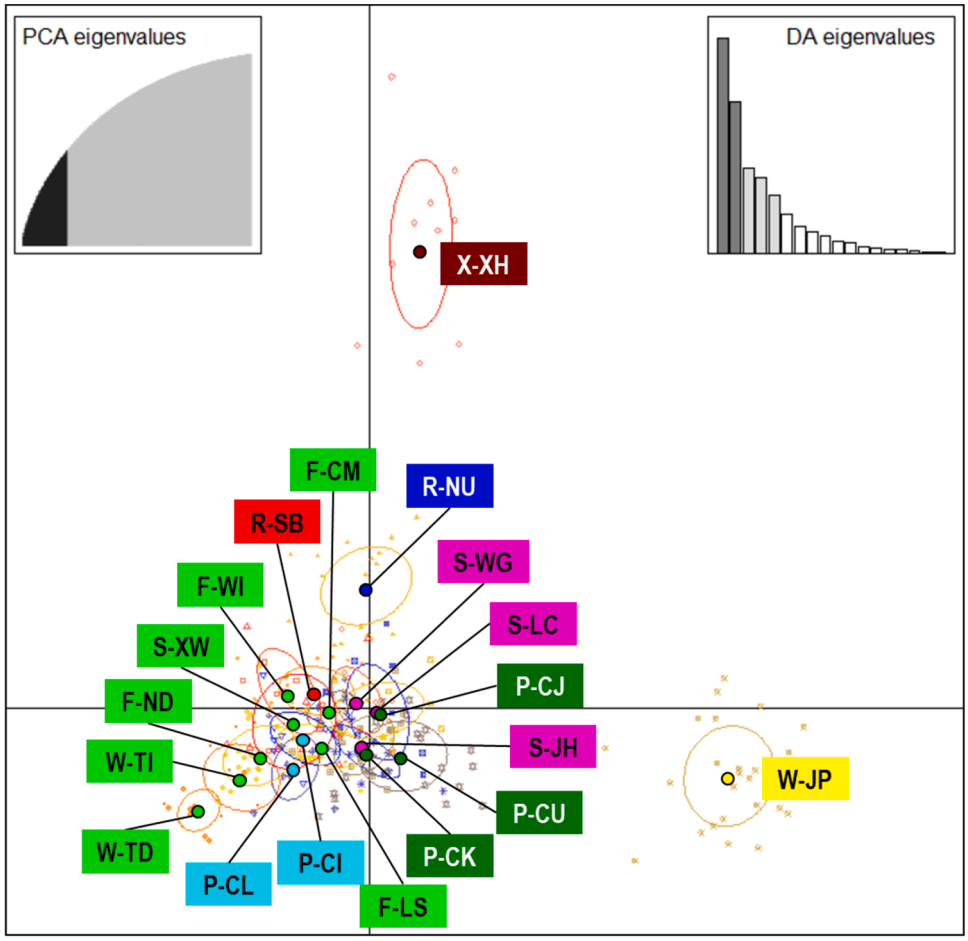

Fig. 3. Discriminant Analysis of Principal Components (DAPC) scatterplot of 19 *H. diversicolor* populations. Small dots represent individuals and inertia ellipses represent populations. Big central dots and labels denoting 19 populations, colors represent eight clades based on STRUCTURE analysis.

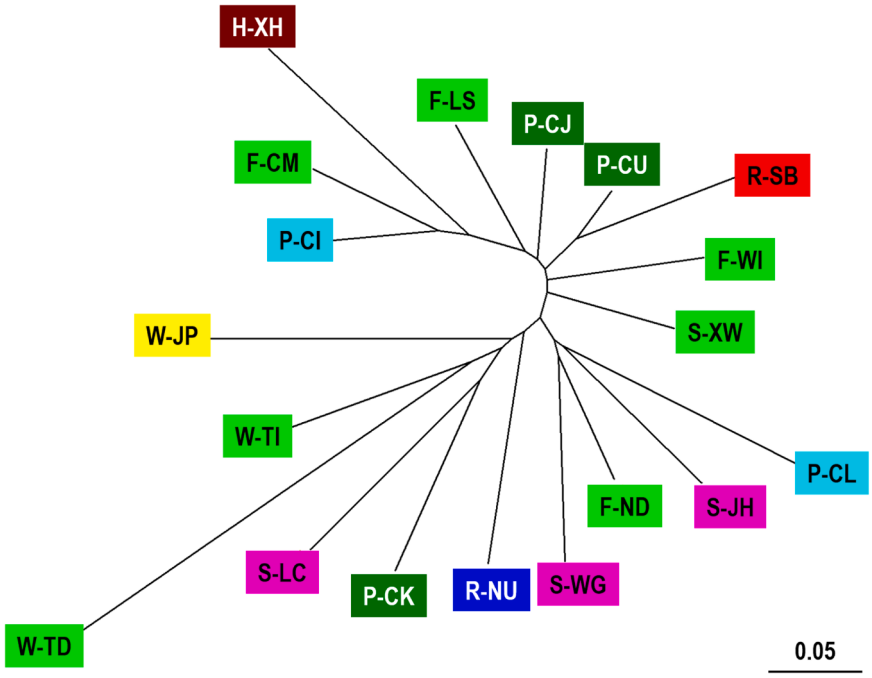

Fig. 4. Phylogenetic tree of 19 *H. diversicolor* populations. Euclidean distance and neighbor-joining method were used. Colors denoting eight clades based on STRUCTURE analysis.

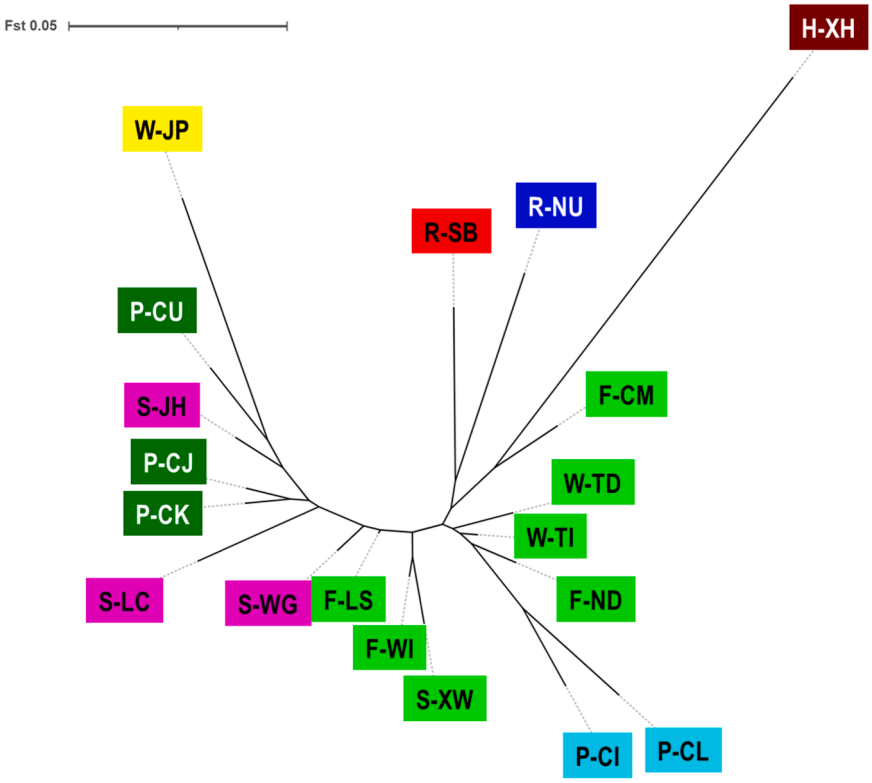

Fig. 5. Phylogenetic tree of 19 *H. diversicolor* populations. F_{ST} distance and neighbor-joining method were used. Colors denoting eight clades based on STRUCTURE analysis.

Although some analyses did not fully support this conclusion, primarily due to their reliance on genetic distance-based methods, STRUCTURE analysis based on admixture models is generally considered more reliable (Lawson et al., 2018). Moreover, based on our prior knowledge, we were confident in distinguishing wild populations from Japan (W-JP), Taiwan-Indonesia hybrids (H-XH), and research breeding program strains (R-SB and R-NU) from commercial strains, a conclusion highly consistent with the results of STRUCTURE analysis. However, through STRUCTURE analysis, we further discovered genetic admixture in private breeding program strain P-CK and commercial hatchery sample

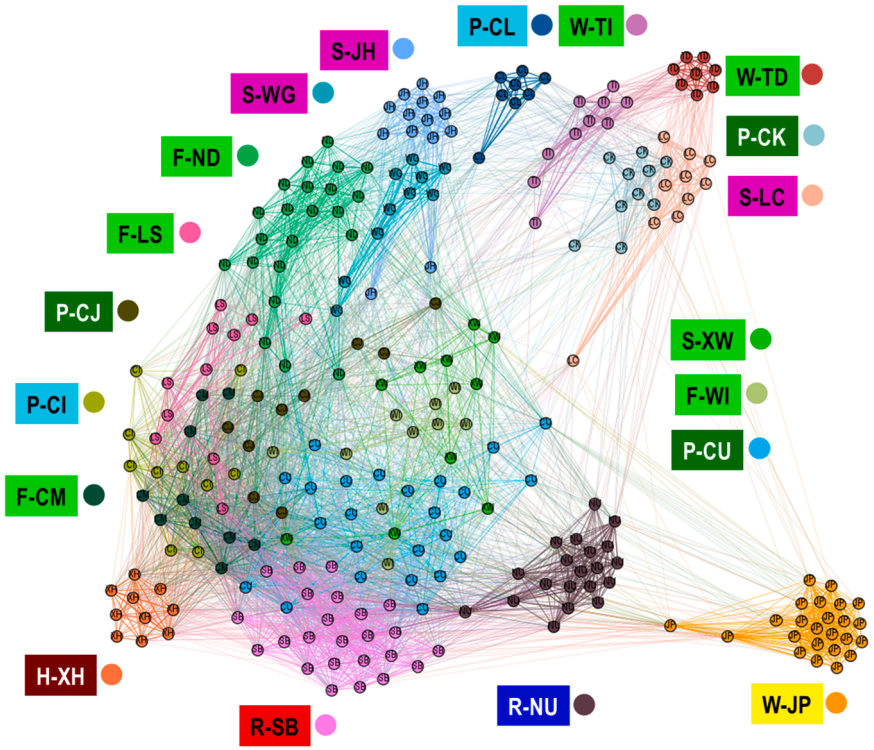

Fig. 6. Relatedness network of 19 *H. diversicolor* populations. Colors of square label denoting eight clades based on STRUCTURE analysis.

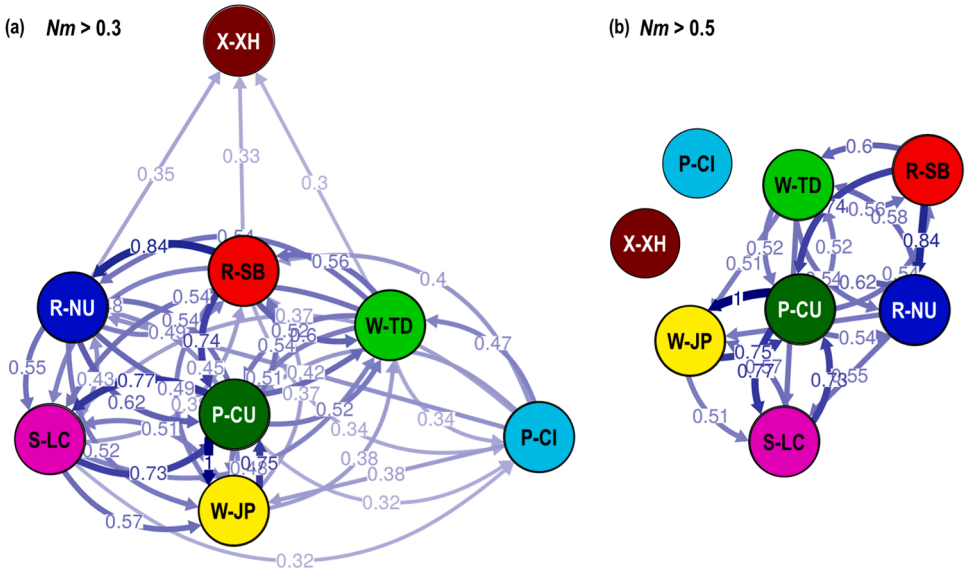

Fig. 7. Relative migration networks for eight major *H. diversicolor* populations (clades). Arrows indicate the putative direction and magnitude of relative migration levels using *Nm*. Darker arrows indicate stronger gene flow compared to lighter arrows. (a) arrows only present when *Nm* > 0.3; (b) arrows only present when *Nm* > 0.5. Colors of circle label denoting eight clades based on STRUCTURE analysis.

S-WG, which was previously unknown. The genetic admixture observed in several commercial farm samples, including F-CM, F-LS, and F-ND, was expected. As we know, many mass culture operators opt to release at least two batches of abalones from different origins to diversify the sources of seedlings. This strategy is adopted because relying solely on seeds from a single source may not ensure the minimum yield after mass mortality. Genetic admixture is also reasonable for wild populations from Taiwan (W-TD and W-TI) due to multiple stock enhancement activities in recent years, where the sources and genetic backgrounds of released seedlings are often uncertain, resulting in genetic introgression.

As for the Taiwan-Indonesia hybrid strain H-XH, multiple backcrosses with Taiwanese stocks have occurred after introducing Indonesian stocks, resulting in a lack of apparent clustering in the STRUCTURE analysis, with most clusters only accounting for approximately 50 % of the results (Fig. 2a). A high degree of exchange (Nm > 0.3) was observed in the gene flow analysis of the eight major clades (Fig. 7a). The gene flow direction for H-XH (Taiwan-Indonesia hybrids) is unidirectional, indicating that H-XH indeed hybridized with other Taiwanese populations. This finding is consistent with the STRUCTURE results and our understanding. Apart from H-XH, the remaining seven major clades

exhibited bidirectional or indirect high gene flow, particularly P-CU, R-NU, R-SB, W-TD, S-LC, and W-JP (Nm > 0.5; Fig. 7b). This result further confirms the high exchange level among farmed abalone in Taiwan and reflects the history of past introductions and long-term releases.

From a spatial perspective, the relatedness network highlights W-JP as the most distinct, signifying significant differences between the populations of Taiwan and Japan (Fig. 6). Around a decade ago, *H. diversicolor* from Japan were introduced to Taiwan for breeding programs. However, Taiwan hatcheries did not consistently maintain pure Japan or Indonesian strains. Instead, they hybridized them with Taiwan stocks and subsequently backcrossed them. Over the past decade, spanning approximately 4–5 generations, this breeding approach has increased genetic distance between W-JP and Taiwanese stocks. Conversely, H-XH, originating from multiple backcrosses of hybrid offspring, demonstrates a high relatedness for Taiwan populations. In the network analysis, most population samples conform to prior information, clustering with individuals from the same source (Fig. 6). However, some individuals exhibit genetic admixture, which is consistent with STRUCTURE analysis, thus bolstering the credibility of both analytical approaches (Figs. 2a and 6). Furthermore, notable high relatedness is observed among wild populations (W-TD and W-TI) in Taiwan, commercial hatchery S-LC, and private breeding program strains P-CK. This suggests that S-LC and P-CK are predominantly derived from Taiwan's wild populations. Industry sources confirm that this can be attributed to long-standing disease issues. In addition to hybridizing with Japanese and Indonesian stocks, some operators have introduced stocks from Taiwan's wild populations to enhance the genetic diversity of commercial strains. Although this hypothesis diverges from the clustering results of STRUCTURE analysis, it remains noteworthy. We contend that spatially distributed network analysis offers more nuanced insights than structural analysis.

Previously, genetic management and parentage identification of abalones primarily relied on SSR markers. However, traditional molecular markers like microsatellites often involve fewer markers and longer development times (Aguilar-Espinoza et al., 2014; Chen et al., 2017; Hsu and Gwo, 2017). Despite efforts to accelerate development speed by obtaining SSR from the genome or transcriptome using NGS, subsequent genotyping still relies on traditional non-high-throughput methods (e.g., capillary electrophoresis) (Gao et al., 2012; Aguilar-Espinoza et al., 2014; Hsu et al., 2021; Chen et al., 2022). Many studies have compared the advantages and disadvantages of SSR and SNP markers, and we specifically focus on the power of both methods for genetic structure (Muñoz et al., 2017; Lemopoulos et al., 2019; Hauser et al., 2021). Based on our past experiences, the resolution of genetic structure in abalones using SSR, mtDNA, and AFLP markers is far inferior to the results obtained using SNP markers in this study, especially when genetic differences are minimal or there is frequent gene flow. The limited number of microsatellite markers may not allow in-depth individual-level analysis (Hsu and Gwo, 2017).

The widespread adoption and decreased cost of high-throughput sequencing technologies have broadened their applications and been successfully employed across multiple species (Yang et al., 2020; Chu et al., 2021; Wong et al., 2022). In our study, the ISSRseq method stands out from other RADseq techniques primarily because it is PCR-based, requiring lower sample DNA quantity and quality (Suyama and Matsuki, 2015; Sinn et al., 2022). The ISSRseq technology utilized in our study enables individual identification by incorporating an index from the primer pair during PCR amplification of each sample, thus significantly reducing the cost of NGS sequencing (Hsu et al., 2024). Despite the increasing prevalence of genome research and the decreasing cost per unit, directly employing re-sequencing-based technology (e.g., low-coverage sequencing for genomic selection) for large-scale studies remains challenging (Zhang et al., 2021; Wong et al., 2022). However, for small-scale applications (with SNP numbers ranging from hundreds to thousands), the workflow of ISSRseq is considerably more straightforward than that of re-sequencing and RADseq-related techniques (Suyama and Matsuki, 2015; Sinn et al., 2022). These advantages render ISSRseq more suitable and efficient for genetic management (Hsu et al., 2024).

Our research underscores the existing gap between practical stock management and genetic management. We have demonstrated that ISSRseq can infer the clade relationships of *H. diversicolor* even without prior genetic and practical information, showcasing its potential for the genetic management and breeding program. Through various analyses, significant differences are found among the Japanese wild population, Taiwan wild populations, Taiwan-Indonesia hybrid strain, and other cultured populations. Selective strains bred by research institutions and private hatcheries exhibit uniqueness distinct from commonly commercial *H. diversicolor*. The presence of multiple populations exhibiting admixture may be attributed to improper stock enhancement and management practices.

Furthermore, although ISSRseq markers, like RADseq, do not require prior genomic information, they can still be mapped to a reference genome when available (Lee et al., 2019; Fujimoto et al., 2022; Hsu et al., 2024). This enables further exploration to determine whether specific SNPs originate from genic regions and are associated with specific gene functions, a potential that may be further exploited in the future (Lee et al., 2019; Fujimoto et al., 2022; Hsu et al., 2024). In summary, Our work elucidates the current status of genetic resources of Taiwan *H. diversicolor*, laying the foundation for future breeding efforts.

Funding

This research is supported by the Fisheries Research Institute, MOA, Taiwan, with grant numbers 111AS-1.6.1-AI-A2, 112AS-6.1.2-AI-A1 and 113AS-6.1.2-AI-02, and Ministry of Education, Taiwan (Featured Areas Research Center Program within the framework of the Higher Education Sprout Project to Center of Excellence for the Oceans, National Taiwan Ocean University).

CRediT authorship contribution statement

Te-Hua Hsu: Writing – review & editing, Writing – original draft, Visualization, Validation, Supervision, Software, Resources, Project administration, Methodology, Investigation, Funding acquisition, Formal analysis, Data curation, Conceptualization. **Fan-Hua Nan:** Supervision, Resources, Funding acquisition. **Yung-Cheng Chang:** Writing – original draft, Methodology, Investigation, Data curation, Conceptualization.

Declaration of Generative AI and AI-assisted technologies in the writing process

Statement: During the preparation of this work we used ChatGPT in order to improve readability and language. After using this tool/service, we reviewed and edited the content as needed and take(s) full responsibility for the content of the publication.

Declaration of Competing Interest

The authors declare the following financial interests/personal relationships which may be considered as potential competing interests: Te-Hua Hsu reports financial support, administrative support, article publishing charges, equipment, drugs, or supplies, travel, and writing assistance were provided by Fisheries Research Institute, MOA, Taiwan. Te-Hua Hsu reports financial support, administrative support, article publishing charges, equipment, drugs, or supplies, travel, and writing assistance were provided by Center of Excellence for the Oceans, National Taiwan Ocean University.

Data availability

Data will be made available on request.

Acknowledgements

The authors extend their gratitude to Mr. Jheng Cing-Huang for providing the *H. diversicolor* strains from the private breeding program. Additionally, we thank Dr. Jin-Lien Du and Fu-shen Tseng (Fisheries Research Institute) for providing us with information on the abalone aquaculture industry and abalone samples (NTOU 108).

References

Aguilar-Espinoza, A., Valderrama-Aravena, N., Farlora, R., Lafarga De la Cruz, F., Gallardo-Escárate, C., 2014. Development of novel polymorphic EST-SSR markers in Californian abalone *Haliotis rufescens* and genetic analysis in wild and hatchery-bred populations. Aquac. Res. 45, 1942–1952. https://doi.org/10.1111/are.12141.

Alexander, D.H., Novembre, J., Lange, K., 2009. Fast model-based estimation of ancestry in unrelated individuals. Genome Res. 19, 1655–1664. https://doi.org/10.1101/gr.094052.109.

An, H.S., Lee, J.W., Kim, H.C., Myeong, J.-I., 2011. Genetic characterization of five hatchery populations of the pacific abalone (*Haliotis discus hannai*) using microsatellite markers. Int. J. Mol. Sci. 12, 4836–4849. https://doi.org/10.3390/ijms12084836.

Andrews, S., 2010. FastQC: a quality control tool for high throughput sequence data. Available online at: http://www.bioinformatics.babraham.ac.uk/projects/fastqc.

Bastian, M., Heymann, S., Jacomy, M., 2009. Gephi: an open source software for exploring and manipulating networks. Proc. Int. AAAI Conf. Web Soc. Media 3, 361–362. https://doi.org/10.1609/icwsm.v3i1.13937.

Bolger, A.M., Lohse, M., Usadel, B., 2014. Trimmomatic: a flexible trimmer for Illumina sequence data. Bioinformatics 30, 2114–2120. https://doi.org/10.1093/bioinformatics/btu170.

Chang, P.H., Kuo, S.T., Lai, S.H., Yang, H.S., Ting, Y.Y., Hsu, C.L., Chen, H.C., 2005. Herpes-like virus infection causing mortality of cultured abalone *Haliotis diversicolor supertexta* in Taiwan. Dis. Aquat. Org. 65, 23–27. https://doi.org/10.3354/dao065023.

Chen, C.-C., Huang, C.-W., Lin, C.-Y., Ho, C.-H., Pham, H.N., Hsu, T.-H., Lin, T.-T., Chen, R.-H., Yang, S.-D., Chang, C.-I., Gong, H.-Y., 2022. Development of disease-resistance-associated microsatellite DNA markers for selective breeding of tilapia (*Oreochromis* spp.) farmed in Taiwan. Genes 13, 99. https://doi.org/10.3390/genes13010099.

Chen, M.H., Kuo, S.T., Renault, T., Friedman, C.S., Chang, P.H., 2012. Development of a polymerase chain reaction for the detection of abalone herpesvirus infection based on the DNA polymerase gene. J. Virol. Methods 185, 1–6. https://doi.org/10.1016/j.jviromet.2012.03.024.

Chen, M.H., Kuo, S.T., Renault, T., Chang, P.H., 2014. The development of a loop-mediated isothermal amplification assay for rapid and sensitive detection of abalone herpesvirus DNA. J. Virol. Methods 196, 199–203. https://doi.org/10.1016/j.jviromet.2013.11.011.

Chen, J., Lee, W., 1999. Growth of Taiwan abalone *Haliotis diversicolor supertexta* fed on *Gracilaria tenuistipitata* and artificial diet in a multiple-tier basket system. J. Shellfish Res. 18.

Chen, N., Luo, X., Lu, C., Ke, C., You, W., 2017. Effects of artificial selection practices on loss of genetic diversity in the Pacific abalone, *Haliotis discus hannai*. Aquac. Res. 48, 4923–4933. https://doi.org/10.1111/are.13311.

Chu, P.-Y., Li, J.-X., Hsu, T.-H., Gong, H.-Y., Lin, C.-Y., Wang, J.-H., Huang, C.-W., 2021. Identification of genes related to cold tolerance and novel genetic markers for molecular breeding in Taiwan tilapia (*Oreochromis* spp.) via transcriptome analysis. Animals 11, 3538. https://doi.org/10.3390/ani11123538.

de Jong, M.J., de Jong, J.F., Hoelzel, A.R., Janke, A., 2021. SambaR: an R package for fast, easy and reproducible population-genetic analyses of biallelic SNP data sets. Mol. Ecol. Resour. 21, 1369–1379. https://doi.org/10.1111/1755-0998.13339.

Degnan, S.M., Imron, Geiger, D.L., Degnan, B.M., 2006. Evolution in temperate and tropical seas: disparate patterns in southern hemisphere abalone (Mollusca: Vetigastropoda: Haliotidae). Mol. Phylogenetics Evol. 41, 249–256. https://doi.org/10.1016/j.ympev.2006.06.023.

Dupanloup, I., Schneider, S., Excoffier, L., 2002. A simulated annealing approach to define the genetic structure of populations. Mol. Ecol. 11, 2571–2581. https://doi.org/10.1046/j.1365-294X.2002.01650.x.

Estes, J.A., Lindberg, D.R., Wray, C., 2005. Evolution of large body size in abalones (*Haliotis*): patterns and implications. Paleobiology 31, 591–606 https://doi.org/10.1666/0094-8373(2005)031[0591:EOLBSI]2.0.CO;2.

Excoffier, L., Lischer, H.E.L., 2010. Arlequin suite ver 3.5: a new series of programs to perform population genetics analyses under Linux and Windows. Mol. Ecol. Resour. 10, 564–567. https://doi.org/10.1111/j.1755-0998.2010.02847.x.

FAO. (2000) *FishStat Plus: Universal software for fishery statistical time series, Version* 2.3. FAO, Rome, Italy.

Fujimoto, S., Yaguchi, H., Myosho, T., Aoyama, H., Sato, Y., Kimura, R., 2022. Population admixtures in medaka inferred by multiple arbitrary amplicon sequencing. Sci. Rep. 12, 19989 https://doi.org/10.1038/s41598-022-24498-7.

Gao, Z., Luo, W., Liu, H., Zeng, C., Liu, X., Yi, S., Wang, W., 2012. Transcriptome Analysis and SSR/SNP Markers Information of the Blunt Snout Bream (*Megalobrama amblycephala*). PLOS ONE 7, e42637. https://doi.org/10.1371/journal.pone.0042637.

Gao, X., Zhang, M., Luo, X., You, W., Ke, C., 2023. Transitions, challenges and trends in China's abalone culture industry. Rev. Aquac. 15, 1274–1293. https://doi.org/10.1111/raq.12769.

L. Geiger, D., 1999. Distribution and biogeography of the recent Haliotidae world-wide.: (Gastropoda: Vetigastropoda). Bollettino Malacologico 57–118.

Gu, L., Qi, R.-J., Yang, R., Han, T., Jiang, J.-Z., Wang, J.-Y., 2019. The prevalence of abalone herpesvirus in two *Haliotis* species in South China during 2002–2013. Aquaculture 505, 18–26. https://doi.org/10.1016/j.aquaculture.2019.02.026.

Hauser, S.S., Athrey, G., Leberg, P.L., 2021. Waste not, want not: Microsatellites remain an economical and informative technology for conservation genetics. Ecol. Evol. 11, 15800–15814. https://doi.org/10.1002/ece3.8250.

Hsu, T.-H., Chiu, Y.-T., Lee, H.-T., Gong, H.-Y., Huang, C.-W., 2021. Development of EST-molecular markers from RNA sequencing for genetic management and identification of growth traits in potato grouper (*Epinephelus tukula*). Biology 10, 36. https://doi.org/10.3390/biology10010036.

Hsu, T.-H., Chu, P.-Y., Gong, H.-Y., Nan, F.-H., Huang, C.-W., 2024. Utilizing ISSRseq genotyping to assist growth selection in tomato grouper (*Cephalopholis sonnerati*) without broodstock information. J. World Aquac. Soc. 55, e13035 https://doi.org/10.1111/jwas.13035.

Hsu, T.-H., Guillén Madrid, A.G., Burridge, C.P., Cheng, H.-Y., Gwo, J.-C., 2011. Resolution of the Acanthopagrus black seabream complex based on mitochondrial and amplified fragment-length polymorphism analyses. J. Fish. Biol. 79, 1182–1192. https://doi.org/10.1111/j.1095-8649.2011.03100.x.

Hsu, T.-H., Gwo, J.-C., 2017. Genetic diversity and stock identification of small abalone (*Haliotis diversicolor*) in Taiwan and Japan. PLOS ONE 12, e0179818. https://doi.org/10.1371/journal.pone.0179818.

Hsu, T.-H., Huang, C.-W., Lee, H.-T., Kuo, Y.-H., Liu, K.-M., Lin, C.-H., Gong, H.-Y., 2020a. Population genetic analysis for stock enhancement of silver sea bream (*Rhabdosargus sarba*) in Taiwan. Fishes 5, 19. https://doi.org/10.3390/fishes5020019.

Hsu, T.-H., Huang, C.-W., Lin, C.-H., Lee, H.-T., Pan, C.-Y., 2020b. Tracing the origin of fish without hatchery information: genetic management of stock enhancement for mangrove red snapper (*Lutjanus argentimaculatus*) in Taiwan. Fish. Aquat. Sci. 23, 13. https://doi.org/10.1186/s41240-020-00156-9.

Hsu, T.-H., Lee, H.-T., Lu, H.-J., Liao, C.-H., Gong, H.-Y., Huang, C.-W., 2022. Maintenance of genetic diversity of black sea bream despite unmonitored and large-scale hatchery releases. Biology 11, 554. https://doi.org/10.3390/biology11040554.

Huang, W.-B., Hseu, J.-R., 2010. Changes in growth characteristics of the small abalone *Haliotis diversicolor* (Reeve, 1846) after one decade in a closed culture system: a comparison with wild populations. Fish. Sci. 76, 131–137. https://doi.org/10.1007/s12562-009-0190-1.

Jiang, J.-Z., Zhu, Z.-N., Zhang, H., Liang, Y.-Y., Guo, Z.-X., Liu, G.-F., Su, Y.-L., Wang, J.-Y., 2012. Quantitative PCR detection for abalone shriveling syndrome-associated virus. J. Virol. Methods 184, 15–20. https://doi.org/10.1016/j.jviromet.2012.04.009.

Jombart, T., Ahmed, I., 2011. adegenet 1.3-1: new tools for the analysis of genome-wide SNP data. Bioinformatics 27, 3070–3071. https://doi.org/10.1093/bioinformatics/btr521.

Kamvar, Z.N., Tabima, J.F., Grünwald, N.J., 2014. Poppr: an R package for genetic analysis of populations with clonal, partially clonal, and/or sexual reproduction. PeerJ 2, e281. https://doi.org/10.7717/peerj.281.

Kopelman, N.M., Mayzel, J., Jakobsson, M., Rosenberg, N.A., Mayrose, I., 2015. Clumpak: a program for identifying clustering modes and packaging population structure inferences across K. Mol. Ecol. Resour., Clumpak 15, 1179–1191. https://doi.org/10.1111/1755-0998.12387.

Lawson, D.J., van Dorp, L., Falush, D., 2018. A tutorial on how not to over-interpret STRUCTURE and ADMIXTURE bar plots. Nat. Commun. 9, 3258. https://doi.org/10.1038/s41467-018-05257-7.

Lee, B.-Y., Kim, M.-S., Choi, B.-S., Nagano, A.J., Au, D.W.T., Wu, R.S.S., Takehana, Y., Lee, J.-S., 2019. Construction of high-resolution RAD-Seq based linkage map, anchoring reference genome, and QTL mapping of the sex chromosome in the marine medaka *Oryzias melastigma*. G3 Genes|Genomes|Genet. 9, 3537–3545. https://doi.org/10.1534/g3.119.400708.

Lemopoulos, A., Prokkola, J.M., Uusi-Heikkilä, S., Vasemägi, A., Huusko, A., Hyvärinen, P., Koljonen, M.-L., Koskiniemi, J., Vainikka, A., 2019. Comparing RADseq and microsatellites for estimating genetic diversity and relatedness — Implications for brown trout conservation. Ecol. Evol. 9, 2106–2120. https://doi.org/10.1002/ece3.4905.

Letunic, I., Bork, P., 2021. Interactive Tree Of Life (iTOL) v5: an online tool for phylogenetic tree display and annotation. Nucleic Acids Res. 49, W293–W296. https://doi.org/10.1093/nar/gkab301.

Li, Y.-L., Liu, J.-X., 2018. StructureSelector: A web-based software to select and visualize the optimal number of clusters using multiple methods. Mol. Ecol. Resour. 18, 176–177. https://doi.org/10.1111/1755-0998.12719.

Li, Q., Shu, J., Yu, R., Tian, C., 2007. Genetic variability of cultured populations of the Pacific abalone (*Haliotis discus hannai* Ino) in China based on microsatellites. Aquac. Res. 38, 981–990. https://doi.org/10.1111/j.1365-2109.2007.01764.x.

Martin, M., 2011. Cutadapt removes adapter sequences from high-throughput sequencing reads. EMBnet. J. 17, 10–12. https://doi.org/10.14806/ej.17.1.200.

Muñoz, I., Henriques, D., Jara, L., Johnston, J.S., Chávez-Galarza, J., De La Rúa, P., Pinto, M.A., 2017. SNPs selected by information content outperform randomly

selected microsatellite loci for delineating genetic identification and introgression in the endangered dark European honeybee (*Apis mellifera mellifera*). Mol. Ecol. Resour. 17, 783–795. https://doi.org/10.1111/1755-0998.12637.

Nie, Z., Wang, S., 2004. The status of abalone culture in China. J. Shellfish Res. 23, 941–946.

Onuki, K., Fuke, Y., 2022. Rediscovery of a native freshwater shrimp, *Neocaridina denticulata*, and expansion of an invasive species in and around Lake Biwa, Japan: genetic and morphological approach. Conserv. Genet. 23, 967–980. https://doi.org/10.1007/s10592-022-01467-1.

Paris, J.R., Stevens, J.R., Catchen, J.M., 2017. Lost in parameter space: a road map for stacks. Methods Ecol. Evol. 8, 1360–1373. https://doi.org/10.1111/2041-210X.12775.

Pew, J., Muir, P.H., Wang, J., Frasier, T.R., 2015. related: an R package for analysing pairwise relatedness from codominant molecular markers. Mol. Ecol. Resour. 15, 557–561. https://doi.org/10.1111/1755-0998.12323.

Puechmaille, S.J., 2016. The program structure does not reliably recover the correct population structure when sampling is uneven: subsampling and new estimators alleviate the problem. Mol. Ecol. Resour. 16, 608–627. https://doi.org/10.1111/1755-0998.12512.

Ramasamy, R.K., Ramasamy, S., Bindroo, B.B., Naik, V.G., 2014. STRUCTURE PLOT: a program for drawing elegant STRUCTURE bar plots in user friendly interface. SpringerPlus 3, 431. https://doi.org/10.1186/2193-1801-3-431.

Rochette, N.C., Rivera-Colón, A.G., Catchen, J.M., 2019. Stacks 2: Analytical methods for paired-end sequencing improve RADseq-based population genomics. Mol. Ecol. 28, 4737–4754. https://doi.org/10.1111/mec.15253.

Sinn, B.T., Simon, S.J., Santee, M.V., DiFazio, S.P., Fama, N.M., Barrett, C.F., 2022. ISSRseq: An extensible method for reduced representation sequencing. Methods Ecol. Evol. 13, 668–681. https://doi.org/10.1111/2041-210X.13784.

Slabbert, R., Bester, A.E., D'Amato, M.E., 2009. Analyses of genetic diversity and parentage within a south African hatchery of the abalone *Haliotis midae* Linnaeus using microsatellite markers. J. Shellfish Res. 28, 369–375. https://doi.org/10.2983/035.028.0220.

Sundqvist, L., Keenan, K., Zackrisson, M., Prodöhl, P., Kleinhans, D., 2016. Directional genetic differentiation and relative migration. Ecol. Evol. 6, 3461–3475. https://doi.org/10.1002/ece3.2096.

Suyama, Y., Matsuki, Y., 2015. MIG-seq: an effective PCR-based method for genome-wide single-nucleotide polymorphism genotyping using the next-generation sequencing platform. Sci. Rep. 5, 16963 https://doi.org/10.1038/srep16963.

Wang, J., 2002. An estimator for pairwise relatedness using molecular markers. Genetics 160, 1203–1215. https://doi.org/10.1093/genetics/160.3.1203.

Wong, L.L., Razali, S.A., Deris, Z.M., Danish-Daniel, M., Tan, M.P., Nor, S.A.M., Ma, H., Min, W., Yantao, L., Asaduzzaman, M., Sung, Y.Y., Liu, Z., Sorgeloos, P., Van de Peer, Y., Afiqah-Aleng, N., 2022. Application of second-generation sequencing (SGS) and third generation sequencing (TGS) in aquaculture breeding program. Aquaculture 548, 737633. https://doi.org/10.1016/j.aquaculture.2021.737633.

Yang, Y., Wu, L., Wu, X., Li, B., Huang, W., Weng, Z., Lin, Z., Song, L., Guo, Y., Meng, Z., Liu, X., Xia, J., 2020. Identification of candidate growth-related SNPs and genes using GWAS in brown-marbled grouper (*Epinephelus fuscoguttatus*). Mar. Biotechnol. 22, 153–166. https://doi.org/10.1007/s10126-019-09940-8.

You, W.-W., Ke, C.-H., Luo, X., Wang, D.-X., 2009. Growth and survival of three small abalone *Haliotis diversicolor* populations and their reciprocal crosses. Aquac. Res. 40, 1474–1480. https://doi.org/10.1111/j.1365-2109.2009.02247.x.

You, X., Shan, X., Shi, Q., 2020. Research advances in the genomics and applications for molecular breeding of aquaculture animals. Aquaculture 526, 735357. https://doi.org/10.1016/j.aquaculture.2020.735357.

Zhang, W., Li, Wanbo, Liu, G., Gu, L., Ye, K., Zhang, Y., Li, Wei, Jiang, D., Wang, Z., Fang, M., 2021. Evaluation for the effect of low-coverage sequencing on genomic selection in large yellow croaker. Aquaculture 534, 736323. https://doi.org/10.1016/j.aquaculture.2020.736323.

Zhang, G., Que, H., Liu, X., Xu, H., 2004. Abalone mariculture in China. J. Shellfish Res. 23, 947–951.